AMERICAN SOCIETY FOR MICROBIOLOGY | Applied and Environmental Microbiology

Spatial Distribution of *Lactococcus lactis* Colonies Modulates the Production of Major Metabolites during the Ripening of a Model Cheese

Clémentine Le Boucher,[a,b,c] Valérie Gagnaire,[a,b] Valérie Briard-Bion,[a,b] Julien Jardin,[a,b] Marie-Bernadette Maillard,[a,b] Gaud Dervilly-Pinel,[c] Bruno Le Bizec,[c] Sylvie Lortal,[a,b] Sophie Jeanson,[a,b] Anne Thierry[a,b]

INRA, UMR1253 Science et Technologie du Lait et de l'Œuf, Rennes, France[a]; Agrocampus Ouest, UMR1253 Science et Technologie du Lait et de l'Œuf, Rennes, France[b]; LUNAM Université, Oniris, Laboratoire d'Étude des Résidus et Contaminants dans les Aliments (LABERCA), USC INRA 1329, Nantes, France[c]

In cheese, lactic acid bacteria are immobilized at the coagulation step and grow as colonies. The spatial distribution of bacterial colonies is characterized by the size and number of colonies for a given bacterial population within cheese. Our objective was to demonstrate that different spatial distributions, which lead to differences in the exchange surface between the colonies and the cheese matrix, can influence the ripening process. The strategy was to generate cheeses with the same growth and acidification of a *Lactococcus lactis* strain with two different spatial distributions, big and small colonies, to monitor the production of the major ripening metabolites, including sugars, organic acids, peptides, free amino acids, and volatile metabolites, over 1 month of ripening. The monitored metabolites were qualitatively the same for both cheeses, but many of them were more abundant in the small-colony cheeses than in the big-colony cheeses over 1 month of ripening. Therefore, the results obtained showed that two different spatial distributions of *L. lactis* modulated the ripening time course by generating moderate but significant differences in the rates of production or consumption for many of the metabolites commonly monitored throughout ripening. The present work further explores the immobilization of bacteria as colonies within cheese and highlights the consequences of this immobilization on cheese ripening.

Lactic acid bacteria (LAB), including *Lactococcus lactis*, are essential agents of cheese manufacturing. They contribute to the formation of the specific flavor and texture of the final cheese product, directly through their metabolic activity or indirectly through the release of enzymes in the cheese matrix after autolysis (1, 2). Their main activities in cheese are (i) to acidify the curd by metabolizing milk lactose into lactic acid as the main end product and (ii) to hydrolyze milk caseins into peptides and free amino acids and subsequently to catabolize amino acids into various flavor compounds. Moreover, some LAB, such as the diacetylactis biovar of *L. lactis* subsp. *lactis*, metabolize citrate into diacetyl (2,3-butanedione) and acetoin (2-hydroxy-3-butanone) (3–6).

LAB, as any bacteria, are immobilized in the cheese fat-protein matrix during the coagulation step. They are thus constrained to develop as bacterial colonies, as shown in different types of cheeses by using scanning electronic microscopy (7–9), confocal laser scanning microscopy (10, 11), and fluorescence *in situ* hybridization (12). For example, the researchers who used the latter technique assessed the spatial distribution of different LAB species in the different parts of Stilton cheese and showed that lactococci, *Lactobacillus plantarum*, and *Leuconostoc* were not equally distributed in the core, veins, and crust of the cheese (12). However, the consequences on cheese ripening of immobilization of bacteria as colonies in cheese have rarely been explored.

The spatial distribution of bacterial colonies is characterized by the size and number of colonies for a given bacterial population within the cheese. Studies on the immobilization of LAB as colonies in milk curd highlighted that different inoculation levels led to different sizes of bacterial colonies (13, 14). Jeanson et al. (14) were the first to provide quantitative experimental data regarding the spatial distribution of bacterial colonies in a model cheese. They showed that (i) one immobilized cell gave one colony, (ii) the same final number of cells was reached regardless of the inoculation level, and (iii) the fewer the colonies, the larger the colonies, and vice versa.

The influence of the spatial distribution of colonies on the ripening of model cheeses containing the same *L. lactis* population, distributed either in few big colonies or in numerous small colonies, was recently studied. Two distinct metabolomes differentiated big- and small-colony cheeses, thanks to an innovative untargeted metabolomic approach that provided a global view (15). Some metabolites modulated by the spatial distribution were identified, such as amino acids, organic acids, and a vitamin. However, this first study did not provide kinetics data (15).

Our objective was to explore the consequences of different spatial distributions of bacterial colonies on the time course of cheese ripening. We hypothesized that different spatial distributions may lead to qualitative or quantitative differences in the metabolites produced during ripening due to different pathways or to different rates of production. Our strategy was to monitor the produc-

Received 14 August 2015 **Accepted** 13 October 2015

Accepted manuscript posted online 23 October 2015

Citation Le Boucher C, Gagnaire V, Briard-Bion V, Jardin J, Maillard M-B, Dervilly-Pinel G, Le Bizec B, Lortal S, Jeanson S, Thierry A. 2016. Spatial distribution of *Lactococcus lactis* colonies modulates the production of major metabolites during the ripening of a model cheese. Appl Environ Microbiol 82:202–210. doi:10.1128/AEM.02621-15.

Editor: C. A. Elkins

Address correspondence to Anne Thierry, anne.thierry@rennes.inra.fr.

Supplemental material for this article may be found at http://dx.doi.org/10.1128/AEM.02621-15.

tion of different soluble and volatile metabolites related to carbon metabolism and proteolysis throughout the ripening of a model cheese. The generated model cheeses were those produced during the study of Le Boucher et al. (15), in which only the spatial distribution of bacterial colonies was modified and not the bacterial growth or acidification kinetics.

MATERIALS AND METHODS

Cheese making, including bacterial strain and growth conditions. The generated model cheeses were those previously produced (15). Briefly, *Lactococcus lactis* subsp. *lactis* biovar diacetylactis LD61 (CIRM-BIA1541, collection of the Centre International de Ressources Microbiennes–Bactéries d'Intérêt Alimentaire, INRA, Rennes, France) was stored at −80°C in 15% (vol/vol) glycerol and precultured three times in reconstituted milk powder (100 g/liter of deionized water) (Difco, Becton Dickinson, Le Pont de Claix, France). Five independent precultures were used to generate 5 biological replicates. For each batch, an overnight culture of *L. lactis* was used to inoculate the cheeses at $\sim 10^5$ CFU · g^{-1}. The model cheeses were made from a 4.2-times-concentrated retentate from the ultrafiltration (UF) of skim milk that was heat treated at 92°C for 15 min. After inoculation, each batch was divided into two parts in order to generate two different spatial distributions of bacterial colonies within the cheeses (small colonies and big colonies), leading to 10 cheeses (5 big- and 5 small-colony cheeses) at each ripening time. The two different spatial distributions were generated by adding the coagulant agent Maxiren 180 (DSM Food Specialties, Seclin, France) at two different times: (i) at 0 h simultaneous with inoculation, i.e., when the population was 1.90×10^5 ($\pm 0.05 \times 10^5$) CFU · g^{-1} of cheese for the big-colony cheeses, or (ii) after 8 h, i.e., when the lactococci had grown to 3.15×10^7 ($\pm 0.04 \times 10^7$) CFU · g^{-1} of cheese for the small-colony cheeses. The pH at the time of renneting was the same in both cases, 6.71 (±0.03). After addition of the coagulant agent and regardless of the targeted spatial distribution, the UF retentate was gently stirred manually for 2 min to homogenize it and then was divided into aliquots to yield cheeses of 14 g. All cheeses were first incubated for 1 h at 30°C after the addition of lactococcal starter, then at 19°C for 23 h, and finally at 12°C for 27 days, regardless of the coagulation time.

Microbial enumerations and pH measurement. Cheese samples were diluted 10-fold (wt/wt) in sterile 2% citrate solution (Carlo-Erba Reagents, Val de Reuil, France). The mixture was blended for 1 min using a laboratory blender (Waring Laboratory Science, Grosseron, Saint-Herblain, France). Serial 10-fold dilutions were prepared using a 0.1% sterile tryptone-salt solution (Biokar Diagnostics, Beauvais, France). For each dilution, two petri dishes of M17 agar (Difco, Becton Dickinson, Le Pont de Claix, France) plus 0.5% lactose were incubated aerobically at 30°C for 2 days. Measurements of pH were performed using a pH meter (inoLab pH level 1; WTW, Weilheim, Germany) and pH electrode (Sentix 41; WTW, Oberbayern, Germany).

Preparation of cheese aqueous extracts. All cheeses were frozen at −80°C until extraction. Cheese samples of 10 g were diluted 4-fold (wt/wt) in boiled deionized water. The mixture was then homogenized for 2 min using an Ultra-Turrax T18 disperser (IKA-Werke GmbH & Co. KG, Staufen, Germany) at 21,500 rpm. The homogenates were centrifuged at 10,000 × *g* for 10 min at 4°C, and the supernatants, also called cheese aqueous extracts, were stored at −80°C until analysis.

Total lactate dehydrogenase activity. Lysis of *L. lactis* in UF model cheeses during ripening was monitored by assaying the activity of an intracellular enzyme, lactate dehydrogenase (LDH), released into the cheese aqueous extracts in 3 biological replicates at 0 h, 8 h, and 1, 2, 6, 13, 20, and 27 days, as previously described (10). Briefly, 0.2 ml of cheese aqueous extract, obtained by centrifugation of a whole 14-g cheese, was diluted 15-fold in Tris-maleate buffer. A positive control was made from intracellular cell extracts of the same strain and used as the first and last sample in all sample series. LDH activity was followed by the decrease in optical density (OD) at 340 nm in the presence of pyruvate, NADH, and fructose 1,6-diphosphate. The results were expressed as units per milliliter of cheese aqueous extract, where one unit is defined as the amount of enzyme that catalyzes the oxidation of 1 μmol of NADH per minute at room temperature.

Observation of membrane integrity by confocal microscopy. A Live/Dead BacLight bacterial viability kit (Invitrogen, Villebon-sur-Yvette, France) was used to visualize the repartition of the live and membrane-compromised bacteria within bacterial colonies. Membrane-permeant SYTO 9, excited at 488 nm and detected at 515 (±15) nm, labels live bacteria, whereas membrane-permeant propidium iodide, excited at 543 nm and detected at 590 (±50) nm, labels membrane-compromised bacteria (16). The cheese samples were analyzed by using an inverted confocal laser scanning microscope (CLSM) (Eclipse-TE2000-C1; Nikon, Champigny-sur-Marne, France). A slice of the model cheese (12 by 12 by 3 mm) was placed on a slide, and an 80-μl drop of the mix of dyes was spread on the sample. It was then incubated at room temperature in the dark for 30 to 60 min before microscopic observation.

Determination of the average diameter and interfacial area of bacterial colonies. The diameters of the colonies were manually measured from CLSM pictures for 25 small colonies and 10 big colonies in cheeses at 26 days. The interfacial area of colonies, *A*, was calculated from experimental data, by considering that (i) each colony is spherical and (ii) the final number of colonies is the number of bacteria at renneting, according to Jeanson et al. (14): $A = 4\pi r^2 I$, where *A* is expressed in micrometer squared per gram of cheese, *r* (μm) is the mean radius of colonies, and *I* (g^{-1}) is the number of colonies per gram of cheese at the time of renneting. The ratio of the interfacial areas of colonies in the small-colony and big-colony cheeses was then calculated as $(r_s^2 \cdot I_s)/(r_b^2 \cdot I_b)$.

Analysis of free amino acids. The free amino acid content was determined after deproteinization of the sample by sulfosalicylic acid (Merck-Eurolab, Grosseron S.A., Saint Herblain, France) as previously described (17). Briefly, samples of aqueous cheese homogenate (1 ml) were treated with 50 mg of sulfosalicylic acid to precipitate the proteins, shaken for 15 s, incubated for 1 h at 4°C, and centrifuged at 5,000 × *g* for 15 min at 4°C to pellet the proteins. The supernatants were filtered through a 0.45-μm-pore-size membrane (Sartorius, Palaiseau, France), and the filtrates were diluted 6-fold with 0.2 mol · $liter^{-1}$ lithium citrate buffer (pH 2.2) prior to injection. Amino acids were analyzed by ion-exchange chromatography using a Pharmacia LKB Alpha Plus amino acid analyzer (Amersham Pharmacia Biotech Europe, Munich, Germany) for 3 out of 5 independent replicates at 0 h, 8 h, and 1, 2, 6, 13, 20, and 27 days.

Analysis of volatile metabolites using GC-MS. Volatile metabolites were analyzed using a Clarus 680 gas chromatograph coupled to a Clarus 600T quadrupole mass spectrometer (GC-MS) (PerkinElmer, Courtaboeuf, France), as previously described (18). A Turbo Matrix HS-40 Trap (PerkinElmer) was used as a headspace sampler. A 2.5-g sample of cheese aqueous extract was placed in a 20-ml PerkinElmer vial. Volatile metabolites were separated on an Elite-5MS capillary column (60 m by 0.25 mm by 1 μm; PerkinElmer), with He as the mobile phase. The initial temperature of the oven was 35°C, maintained for 5 min. The increase in temperature was performed at a rate of 7°C per minute up to 140°C and then at 13°C per minute up to 280°C. The mass spectrometer was operated in the scan mode within a mass range of *m/z* 25 to 300, with a scan time of 0.3 s. Ionization was done by electronic impact at 70 eV. GC-MS data were processed using XCMS and the R statistical language, as previously described (18). Volatile metabolites were analyzed for 4 replicates at 0 h, 8 h, and 1, 2, 6, 13, 20, and 27 days.

Analysis of organic acids and sugars using HPLC. For determination of sugars and organic acids, aqueous cheese homogenates from 0 h to 2 days were diluted 5-fold in H_2SO_4, and those from 13 to 27 days were diluted 3-fold in H_2SO_4, with the H_2SO_4 concentration adjusted to reach a final concentration of 5 mmol · $liter^{-1}$ in the samples. After a 30-min centrifugation (10,000 × *g* at 4°C), the proteinous pellet was discarded, and the supernatant was collected to determine the lactose, galactose, lactate, citrate, acetate, and pyruvate concentrations by high-perfor-

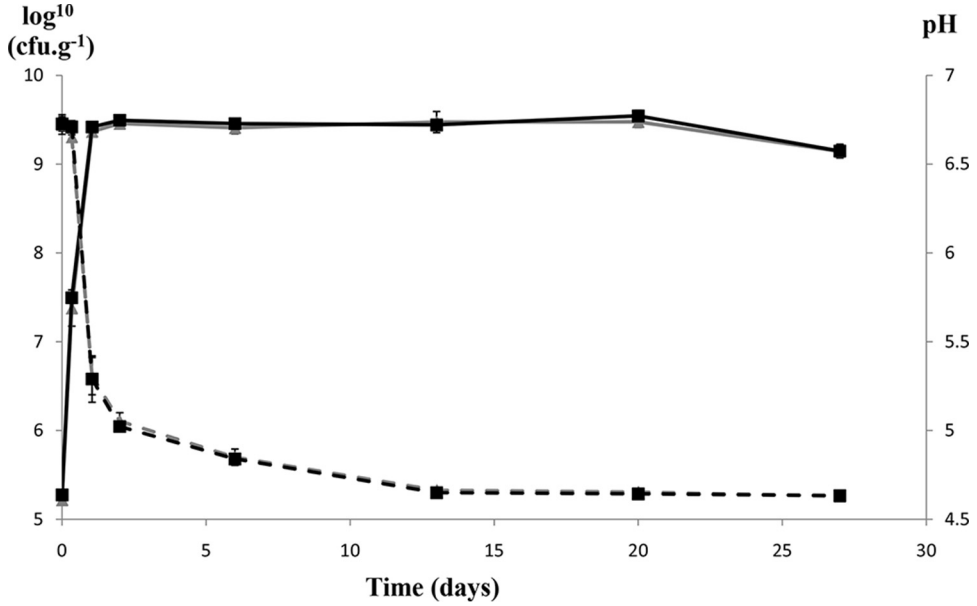

FIG 1 Changes in pH (dashed lines) and in the cultivable population (solid lines) of *Lactococcus lactis* LD61 in small-colony cheeses (■) and big-colony cheeses (▲) incubated at 30°C for 1 h, then at 19°C for 24 h, and finally at 12°C until 27 days of ripening. Values are means of independent replicates ($n = 3$). Bars show standard deviations.

mance liquid chromatography (HPLC) on an Aminex A-6 ion-exchange column (Bio-Rad, Hercules, CA) at 60°C with 0.005 mol · liter^{-1} H_2SO_4 as the eluent at a flow rate of 0.4 ml · min^{-1}. Both UV (210 nm) and refractometric detectors were used. HPLC analyses were performed on 3 out of the 5 independent replicates at 0 h, 8 h, and 1, 2, 13, and 27 days.

Analysis of peptides using nano-liquid chromatography-tandem mass spectrometry (nanoLC-MS/MS). Peptides were analyzed using an RSLCnano Dionex U3000 system fitted to a Q Exactive mass spectrometer (Thermo Scientific, San Jose, CA) equipped with a nanoelectrospray ion source adapted from Lecomte et al. (19), except that 5% to 60% of solvent B in 46 min and 60% to 80% in 1 min were applied as a separation gradient at a flow rate of 0.3 μl · min^{-1}. The analysis was performed on 5 independent replicates at 2, 13, and 27 days. To identify peptides, all data (MS and MS/MS) were submitted to X! Tandem using the X! Tandem pipeline developed by Pappso (http://pappso.inra.fr; Plateforme d'Analyze Protéomique de Paris Sud-Ouest, INRA, Jouy-en-Josas, France). The search was performed against an in-house database, dealing with major milk proteins, that represents a portion of the Swissprot database (http://www.expasy.org). Database search parameters were specified as follows: no enzyme cleavage was used, and the peptide mass tolerance was set to 10 ppm for MS and 0.05 Da for MS/MS. Oxidation of methionine and phosphorylation on threonine and serine were selected as variable modifications. For each identified peptide, a minimum score corresponding to an E value of <0.05 was considered a prerequisite for peptide validation.

Statistical analysis. Repeated analysis of variance (ANOVA) measures were performed on bacterial counts; pH values; concentrations of organic acids, sugars, and free amino acids; and abundance values of volatile metabolites using the R statistical language (http://www.r-project.org/). Due to the presence of high numbers of undetected peptides generating null values, data on the abundance of peptides were subjected to a Peto-Peto's log rank test applied on log-transformed data using the cendiff function of the NADA (Nondetects and Data Analysis) package of R (http://cran.r-project.org/web/packages/NADA/NADA.pdf, by Lopaka Lee and Dennis Helsel).

RESULTS

Growth, acidification, and survival of *L. lactis*. The kinetics of growth and acidification, followed from 0 h to 27 days, did not significantly differ between small- and big-colony cheeses ($P = 0.08$ and 0.79 for CFU and pH, respectively). Low standard deviations within cheese groups showed a high repeatability between the 5 biological replicates (Fig. 1). Growth and acidification mainly occurred between 8 and 24 h. The pH reached 5.30 (±0.11) at 24 h and then slowly decreased for 13 days to reach a final pH of 4.63 (±0.01) in both types of cheeses. The cultivable lactococcal population increased from 1.8×10^5 (±0.2) CFU · g^{-1} of cheese to 2.5×10^9 (±0.3) CFU · g^{-1} at 24 h. It reached a plateau of 3.0×10^9 CFU · g^{-1} and then slightly decreased to 1.4×10^9 (±0.2) CFU · g^{-1} at 27 days of ripening regardless of the spatial distribution. The survival of *L. lactis* was further evaluated from Live/Dead observations, which showed that the cell integrity was preserved from 2 to 27 days of ripening in small- and big-colony cheeses (Fig. 2). Only a few red cells (impaired membrane) randomly dispersed within colonies were visible on some CLSM images. Furthermore, the level of LDH activity remained undetectable (<0.05 units · ml^{-1} · min^{-1}) from 2 to 27 days, while the activity in the positive control (intracellular extract of the same strain) was >2.5 units · ml^{-1} · min^{-1}. These results demonstrate that *L. lactis* cells survived within the UF model cheese from 2 to 27 days of ripening, with no detectable lysis.

Characterization of the two different spatial distributions and calculation of the interfacial area. The two spatial distributions of bacterial colonies appeared clearly differentiated on confocal microscopy pictures (Fig. 2). The average diameter of the colonies was 7.8 (±0.4) μm for small-colony cheeses and 46.2 (±0.4) μm for big-colony cheeses at 27 days. From these values, the interfacial area of colonies was estimated for each spatial distribution and their ratio calculated as equal to 5.4. This means that

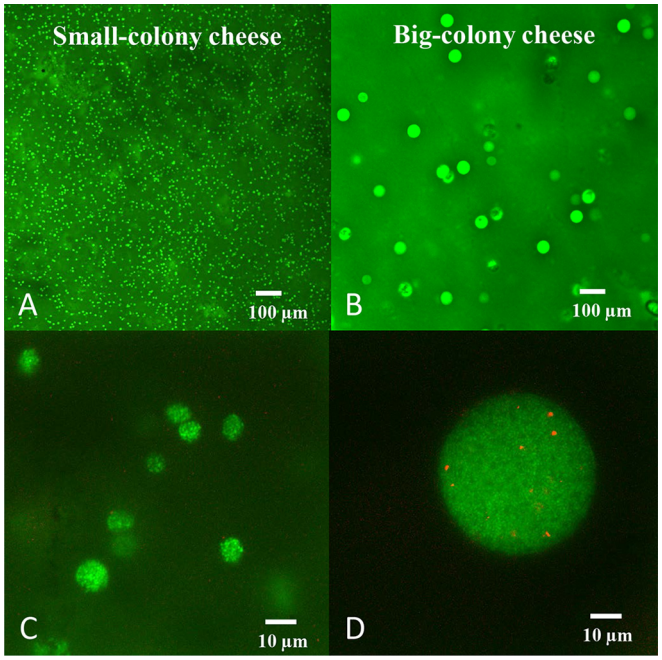

FIG 2 Confocal scanning laser microscope images of model cheeses with two different spatial distributions of bacterial colonies, small-colony (A, C) and big-colony (B, D) cheeses, taken at two different zooms. Ultrafiltered model cheeses were inoculated with *Lactococcus lactis*. Images were taken after 13 days of incubation. Labeling was obtained by combining SYTO 9 (which labels live bacteria [green]) and propidium iodide (which labels membrane-compromised bacteria [red]) (Live/Dead BacLight labeling).

the surface of bacteria in contact with the protein network was about five times larger in the small-colony cheeses than in the big-colony cheeses for the same final bacterial population in all cheeses.

Organic acids and sugars. All the measured organic acids and sugars were detected in both types of cheeses. The concentration of lactose was divided by 2 between 0 and 27 days (Fig. 3), decreasing from 49.0 (±7.8) to 25.4 (±4.4) g · kg^{-1} of cheese in both cheeses, and citric acid was metabolized from the start of the ripening period until exhaustion at 13 days (Fig. 3). The spatial distribution significantly modulated the abundance of three metabolites during the ripening period, which showed higher concentrations in small-colony cheeses than in big-colony cheeses. The concentrations of lactic and pyruvic acids increased during ripening and were significantly higher in small-colony than in big-colony cheeses only at some ripening time points (Fig. 3). Moreover, galactose was detectable from 13 days until the end of ripening, and its concentration was higher in small-colony than in big-colony cheeses (Fig. 3). The ratio of concentrations of these metabolites in small- and big-colony cheeses ranged from 1.33 to 2.04 (small/big), depending on the ripening time and on the measured metabolites.

Free amino acids (FAAs). Throughout the ripening process, 23 FAAs were detected in both small- and big-colony cheeses. The concentration of total FAAs increased in all cheeses from 0 h to 27 days. FAAs accumulated at significantly higher concentrations in small-colony cheeses than in big-colony cheeses (Fig. 4). The con-

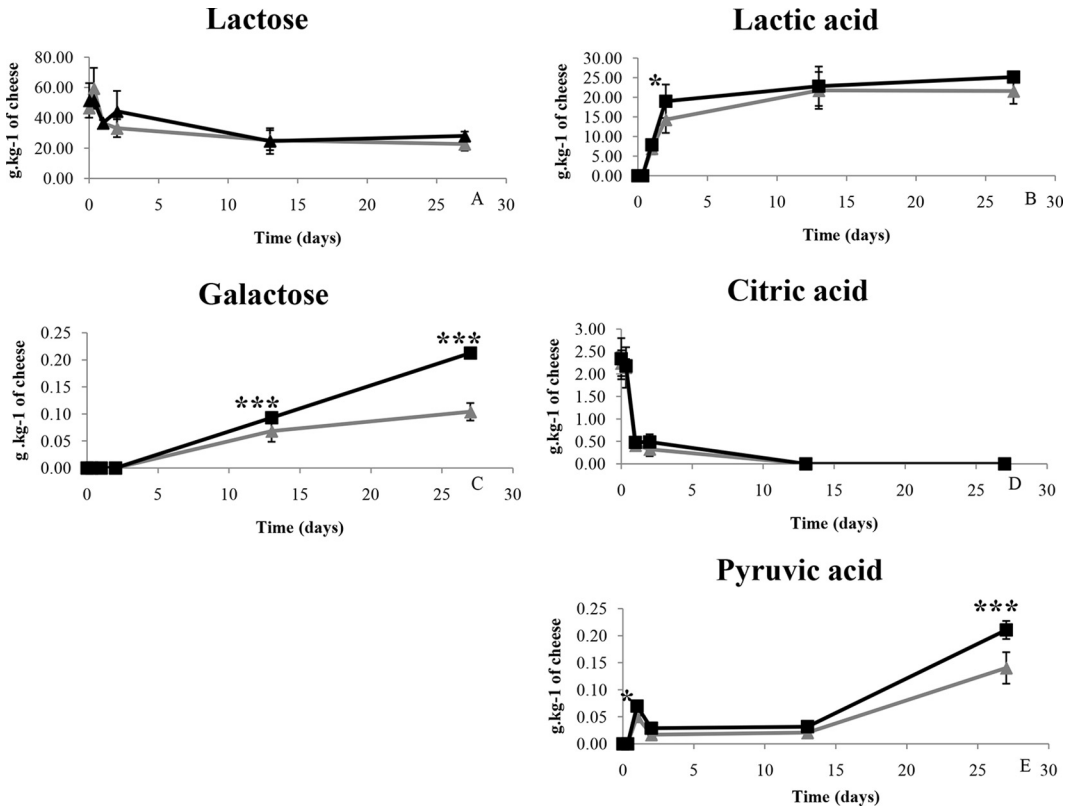

FIG 3 Concentrations of lactose, lactic acid, galactose, citric acid, and pyruvic acid in small-colony cheeses (■) and big-colony cheeses (▲) during ripening. Values are means of independent replicates ($n = 3$). Bars show standard deviations. * and *** indicate significant differences at P values of <0.05 and <0.001, respectively, between big-colony cheeses and small-colony cheeses.

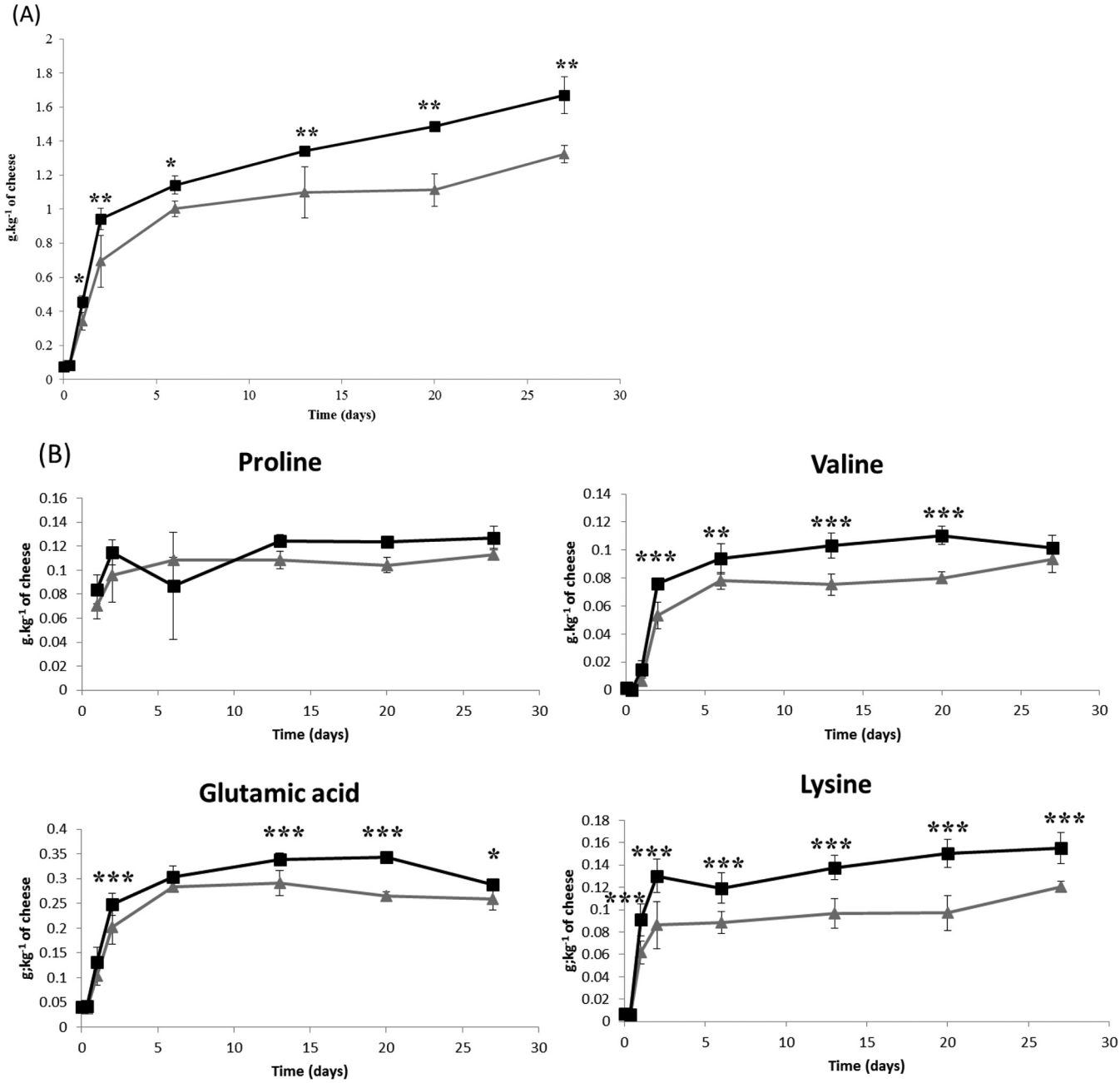

FIG 4 Concentrations of total free amino acids (A) and four individual amino acids (B) in small-colony cheeses (■) and big-colony cheeses (▲) during ripening. Values are means of independent replicates ($n = 3$). Bars show standard deviations. *, **, and *** indicate significant differences at P values of <0.05, <0.01, and <0.001, respectively, between big-colony cheeses and small-colony cheeses.

centration of half of the FAAs and derived amino acid products was globally higher in small-colony than in big-colony cheeses during the whole ripening period (Fig. 4; see also Table S1 in the supplemental material), with statistically significant differences detected throughout ripening for the most abundant FAAs. From 1 to 27 days, the ratio of concentrations of each FAA between small- and big-colony cheeses ranged from 1.04 to 4.11.

The four most abundant amino acids in caseins, i.e., glutamic acid, valine, lysine, and proline, increased in concentration throughout ripening, especially between 8 h and 2 days (Fig. 4). The concentrations of glutamic acid, valine, and lysine were significantly higher in small-colony cheeses than in big-colony cheeses from 2 to 20 days, whereas the differences in proline concentration were not significant. Finally, arginine was not detectable anymore in both cheeses from 6 days of ripening, while two products of arginine conversion, ornithine and citrulline, were present at significantly higher concentrations in small-colony than in big-colony cheeses from 13 days until the end of ripening (see Table S1 in the supplemental material).

Peptides. The total number of peptides identified was 1,400,

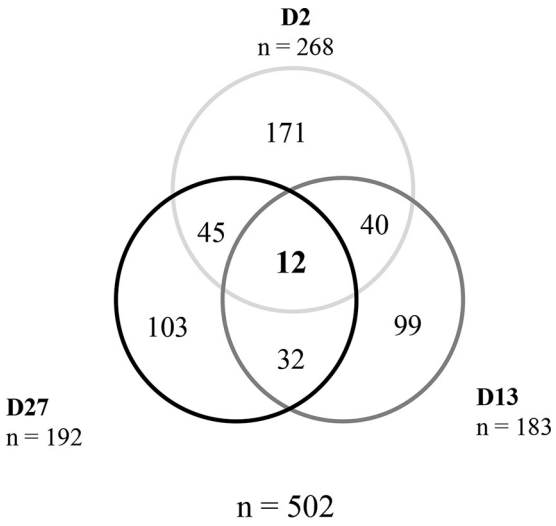

FIG 5 Venn diagram representing the repartition of total discriminant peptides ($P < 0.05$; concentration ratio, >1.2, between small- and big-colony cheeses) at three ripening time points (2, 13, and 27 days).

among which 79.4% were detected at the three time points, meaning that most of the generated peptides were already present at 2 days. The length of the identified peptides ranged from 6 (limit of detection) to 45 amino acid residues, with mainly small peptides up to 15 residues. Peptides were identified from the four milk caseins (β-, α_{s1}-, α_{s2}-, and κ-caseins).

Out of the 1,400 peptides, 502 were significantly modulated by the spatial distribution at least at one time point during the ripening period ($P < 0.05$; concentration ratio, >1.2 between small- and big-colony cheeses). These peptides are also called discriminant peptides. Most of these peptides were discriminant at only one time point, and only 5.7% of them were discriminant at all the time points (Fig. 5). The proportion of discriminant peptides decreased during ripening, from 22.1% to 14.7% between 2 and 27 days (Fig. 6). At 2 days, 98.5% of the discriminant peptides were more abundant in the small-colony than in the big-colony cheeses, after which this proportion decreased to 41.5% and 52.6% at 13 and 27 days, respectively (Fig. 6). The proportion of discriminant peptides differed according to the casein from which they originated. Only 19.8% of the peptides originating from α_{s1}-casein were discriminant, while the proportions of discriminant peptides were higher for the other caseins, with 43.5%, 40%, and 44.9% of the peptides originating from β-, α_{S2}-, and κ-caseins, respectively.

Volatile metabolites. A total of 23 volatile metabolites were identified in both types of cheeses, and all except three (hexanal, heptanol, and nonanal) increased in abundance throughout the ripening period in all cheeses (see Table S2 in the supplemental material). The spatial distribution influenced the accumulation of many volatile metabolites, with significant differences depending on the ripening time and on the volatile metabolite (see Table S2). The more the ripening process was advanced, the higher the number of volatile metabolites that were modulated by the spatial distribution throughout the ripening time. Ten out of 15 volatile metabolites modulated by the spatial distribution, such as diacetyl and acetoin, were more abundant in small-colony cheeses than in big-colony cheeses (Fig. 7). The ratios of abundance of the discriminant ($P < 0.05$; concentration ratio, >1.2, between small- and big-colony cheeses) volatile metabolites in both types of cheeses ranged from 1.2 to 2.2, depending on the ripening time and the volatile metabolite.

DISCUSSION

The present study succeeded in exploring the consequences of the spatial distribution of bacterial colonies on cheese ripening by pointing out the production of metabolites that were modulated by the spatial distribution.

Our model cheese was shown to be relevant to reach this aim. It was chosen to emphasize differences in bacterial activity during ripening in the absence of any lysis of *L. lactis*, confirming previous

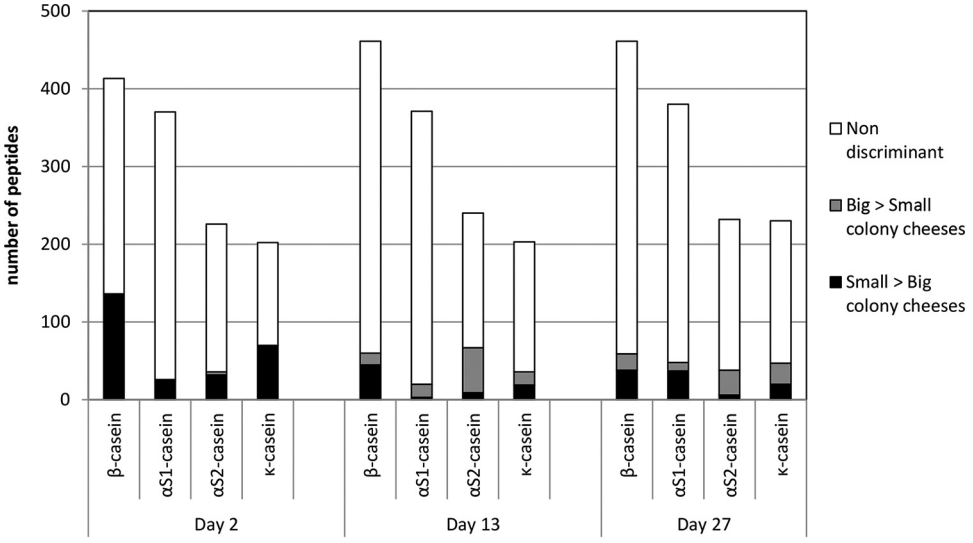

FIG 6 Number of peptides identified per type of casein at three ripening time points (2, 13, and 27 days) and effect of spatial distribution on the peptides. Number of nondiscriminant peptides (white) and number of discriminant peptides ($P < 0.05$; concentration ratio, >1.2, between small- and big-colony cheeses) with an abundance superior in big-colony cheeses (Big > Small colony cheese) or small-colony cheeses (Small > Big colony cheese).

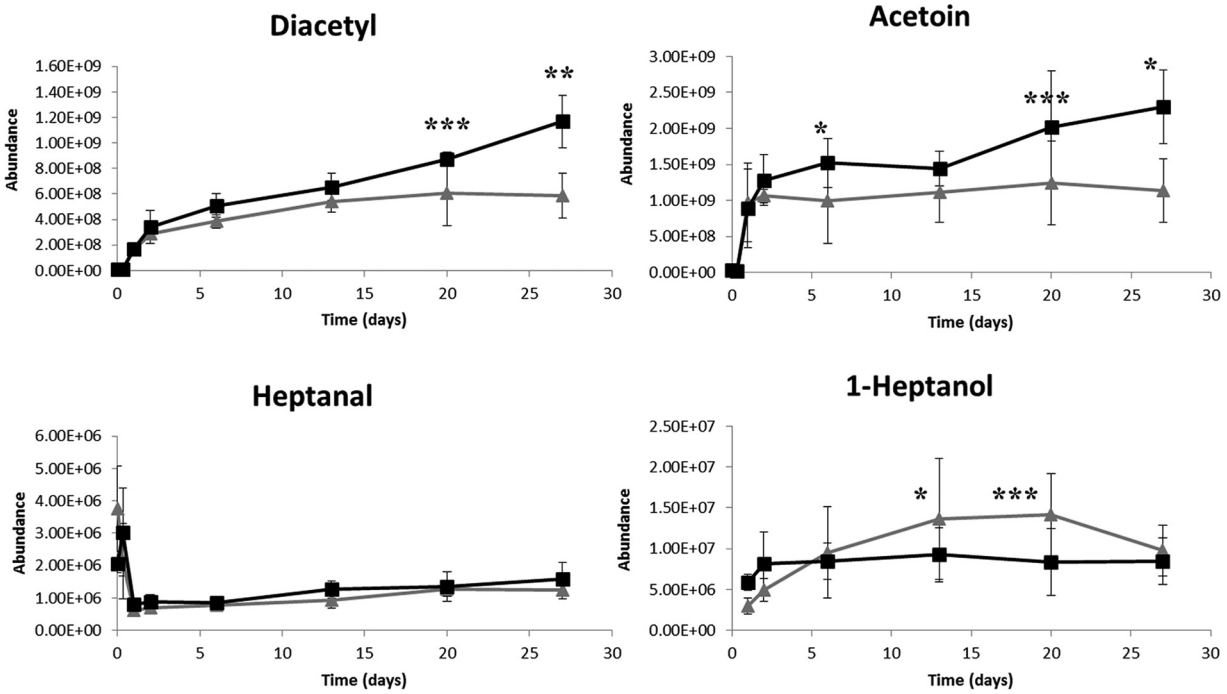

FIG 7 Abundance of diacetyl, acetoin, heptanal, and 1-heptanol in small-colony cheeses (■) and big-colony cheeses (▲) during ripening. Values are means of independent replicates ($n = 4$). Bars show standard deviations. *, **, and *** indicate significant differences at P values of <0.05, <0.01, and <0.001, respectively, between big-colony cheeses and small-colony cheeses.

observations (17). We can thus conclude that (i) the measured metabolites directly resulted from the activity of live bacterial cells and not from the activity of the enzymes that would have been released from lysed cells, and (ii) the differences in the metabolite concentrations observed between small- and big-colony cheeses can directly and exclusively be attributed to the difference in the spatial distributions. Moreover, we used a nonfat cheese because colonies in this cheese are more spherical and dense than colonies formed in a cheese containing fat. This allowed the calculation of experimental values of the interfacial area between the bacterial colonies and the cheese matrix. Therefore, our strategy of a UF model cheese inoculated with *L. lactis* and renneted at two different times was validated as a robust model for determining which metabolites are influenced by the spatial distribution throughout ripening.

The two spatial distributions were distinguished by quantitative but not qualitative differences. The quantified metabolites were related to proteolysis or carbohydrate metabolism and were expected in a ripened cheese (2), including in UF cheeses (10, 17). Indeed, half of the amino acids were present at a significantly higher concentration in small-colony cheeses than in big-colony ones, including (i) major amino acids of caseins, such as glutamic acid, lysine, valine, and alanine; (ii) minor amino acids, such as histidine, tyrosine, and glycine; and (iii) metabolism-derived amino acids, such as citrulline and ornithine produced from the conversion of arginine (see Table S1 in the supplemental material). The ratios of concentrations of metabolites in small- and big-colony cheeses were of the same order of magnitude for peptides and amino acids (from 1 to 5). The larger amount of amino acids in small-colony cheeses indicates a global higher proteolytic activity when the colonies are smaller. Furthermore, the higher concentrations of end products of carbon metabolism, such as galactose, diacetyl, and acetoin, observed in the small-colony cheeses confirm that the bacterial cells forming small colonies use the same metabolic pathways but display a higher metabolic activity than those in big colonies.

Two main phenomena may explain the consequences of different spatial distributions of colonies on the ripening process: (i) the interfacial area, i.e., the exchange surface that exists between all of the bacterial colonies and the cheese matrix, and (ii) the diffusion phenomena within the cheese matrix and within the bacterial colonies. These phenomena are developed below.

The first phenomenon is the interfacial area, determined by the spatial distribution of colonies, as first pointed out by Jeanson et al. (14). Indeed, for the same final bacterial population, a distribution of numerous small colonies displays a larger interfacial area than a population of a few big colonies. In the present study, the interfacial area was 5.4-fold larger in small-colony cheeses than in big-colony cheeses. A larger number of cells are thus in contact with the casein matrix in small-colony cheeses. To sustain its growth, *L. lactis* synthesizes a cell wall protease, PrtP, which hydrolyzes caseins into peptides, whereas the peptides produced are further hydrolyzed into smaller peptides and amino acids by intracellular peptidases (20). In small-colony cheeses, a larger number of cell wall PrtP enzymes are in contact with the casein matrix, thus potentially promoting the proteolytic activity of *L. lactis*. This hypothesis is supported by the larger amounts of peptides and amino acids that were observed in small-colony cheeses. Moreover, proteolysis was also qualitatively modulated, with differences between the caseins. It may be related to the accessibility of the caseins within the matrix, as the β-casein can be released more easily in the matrix than the α_{s1}-casein (21).

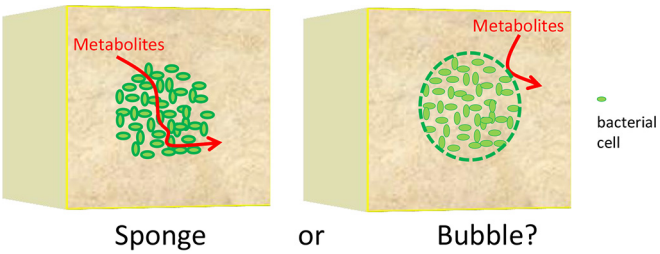

FIG 8 Schematic representation of two bacterial colonies in a solid food matrix according to their ability to act as a sponge or a bubble. Red arrows schematize the diffusion of metabolites, and the green dotted line indicates the interfacial area between the colony and the matrix.

The second phenomenon addresses the question of how the metabolites can diffuse in the colonies. Two extreme conceptions of the bacterial colony can be drawn: the sponge and the bubble (24). In the sponge conception, the colony is porous to the metabolites without limitation of diffusion, and thus all the cells have the same access to nutrients (Fig. 8). Consequently, each cell would equally participate in the ripening process of the cheese regardless of its position within the colony, and the spatial distribution would not induce any change in the production of bacterial metabolites. This means that the ratio of concentrations of metabolites between small- and big-colony cheeses would be equal to 1. A ratio of 1 was observed, for example, for proline, acetic acid, and many peptides, meaning that the spatial distribution of bacterial colonies did not influence their production. In the bubble conception, the bacterial colony is not porous to any metabolite, leading to a slowdown in the metabolism of inner cells compared to that in peripheral cells that actively participate in the cheese-ripening mechanisms (Fig. 8). In this case, the higher the interfacial area, the higher the expected bacterial activity on the cheese matrix. Consequently, smaller colonies would lead to a significant acceleration in cheese ripening, with an expected ratio of concentrations equal to the ratio of interfacial areas between small and big colonies (5 in the present study), indicating diffusion limitations inside the colony. In a few cases, such as for peptides, a ratio of abundance of $\geq$5 was observed, suggesting diffusion limitations of their precursors into the center of the colony.

However, neither of these extreme conceptions is fully supported by the results obtained in this study, since the ratios of concentrations ranged from 1 to 5 for most of the metabolites, confirming the ratios previously observed in the same cheeses by use of an untargeted approach (15). In fact, the bacterial colony can be compared to a selective system, covering all of the possibilities that would be between our two extreme conceptions. Indeed, metabolites would diffuse inside the colonies, with potential limitations depending on the physicochemical properties of the metabolites, the bacterial surface properties, and/or the physicochemical conditions of the cheese. It was observed that dextrans up to 155 kDa could diffuse inside the bacterial colony (22), while three tested proteins, i.e., α_{s1}-casein, lactoferrin, and bovine serum albumin, did not (23), suggesting that the diffusion of metabolites inside the colony depends on intrinsic properties of the metabolites, including their molecular weight, shape, flexibility, and global charge. As potential limitations of diffusion may occur, the bacterial colony may act at the same time as a sponge with no limits of diffusion, a bubble with no diffusion, or a selective system with limited diffusion, depending on the metabolites considered.

The present work demonstrates that the spatial distribution, i.e., the size and number of bacterial colonies, has a moderate but significant effect on the kinetics of ripening. Cells distributed as small colonies close to each other displayed higher global activity, resulting in higher concentrations of some metabolites, related to proteolysis or carbohydrate hydrolysis, in the small-colony cheeses than in the big-colony cheeses. The question remains regarding the mechanisms that fully explain the consequences of the spatial distribution on the ripening process. Further studies are needed to investigate how cells in the center of the colony access their substrates, especially nitrogen substrates.

The potential impact of spatial distribution of the lactic starter on ripening mainly concerns internal bacterially ripened cheeses, in which starters are determinant contributors to proteolysis. In these types of cheeses, an acceleration of proteolysis can be expected from an increase in the starter inoculation level, which would lead to smaller colonies within the cheese matrix. It should be noted that to increase the interfacial area by a factor of 5, as done in the present study, in a classic cheese-making process, it would be necessary to increase the inoculation levels by >2 log CFU $\cdot$ ml^{-1}, which exceeds the range of inoculation levels generally used for lactic starters. Of course, it would also shorten the acidification time course, thereby modifying the entire process. Hence, the reported findings would be relevant in the context of new product development.

In conclusion, the present work lays down the foundation for exploration of the immobilization of bacteria as colonies within cheeses and the consequences on cheese ripening. The UF model cheese chosen here is relevant to the study of cheese ripening. Fat may now be added in combination with a more lipolytic bacterial species than *L. lactis* to investigate the consequences of spatial distribution on lipolysis and on the final sensory properties of cheese. This type of investigation is of major importance for all of the fermented solid foods or other microbial ecosystems, such as soil, in which bacteria grow as colonies.

ACKNOWLEDGMENTS

We are grateful to Pascal Pachot (Stat-plan) for his support with statistical analysis using R software.

FUNDING INFORMATION

This work was performed in the framework of the CheeseOmic project, cofunded by the Brittany and Pays-de-la-Loire Regional Councils (France), and supported by the Bretagne Biotechnologie Alimentaire (Bba) Association. C.L.B. received a Ph.D. grant from the French Ministry of Research.

REFERENCES

1. **Beresford T, Williams A.** 2004. The microbiology of cheese ripening, p 287–317. *In* Fox PF, McSweeney PLH, Cogan TM, Guinee TP (ed), Cheese: chemistry, physics and microbiology, 3rd ed, vol 1. Elsevier Academic Press, Amsterdam, Netherlands.
2. **McSweeney PLH.** 2004. Biochemistry of cheese ripening. Int J Dairy Technol **57:**127–144. http://dx.doi.org/10.1111/j.1471-0307.2004.00147.x.
3. **Smit G, Smit BA, Engels WJ.** 2005. Flavour formation by lactic acid bacteria and biochemical flavour profiling of cheese products. FEMS Microbiol Rev **29:**591–610. http://dx.doi.org/10.1016/j.fmrre.2005.04.002.
4. **Starrenburg MJC, Hugenholtz J.** 1991. Citrate fermentation by *Lactococcus* and *Leuconostoc* spp. Appl Environ Microbiol **57:**3535–3540.
5. **Upadhyay VK, McSweeney PLH, Magboul AAA, Fox PF.** 2004. Proteolysis in cheese during ripening, p 391–433. *In* Fox PF, McSweeney PLH, Cogan TM, Guinee TP (ed), Cheese: chemistry, physics and microbiology, 3rd ed, vol 1. Elsevier Academic Press, Amsterdam, Netherlands.

6. **Yvon M, Rijnen L.** 2001. Cheese flavour formation by amino acid catabolism. Int Dairy J **11:**185–201. http://dx.doi.org/10.1016/S0958-6946(01)00049-8.
7. **Marcellino N, Benson DR.** 1992. Scanning electron and light microscopic study of microbial succession on Bethlehem St-Nectaire cheese. Appl Environ Microbiol **58:**3448–3454.
8. **Parker ML, Gunning PA, Macedo AC, Malcata FX, Brocklehurst TF.** 1998. Microstructure and distribution of micro-organisms within mature Serra cheese. J Appl Microbiol **84:**523–530. http://dx.doi.org/10.1046/j.1365-2672.1998.00375.x.
9. **Rousseau M, Le Gallo C.** 1990. Scanning electron microscopy study of the structure of Emmental cheese during manufacture. Lait **70:**55–66. (In French.) http://dx.doi.org/10.1051/lait:199016.
10. **Hannon JA, Lopez C, Madec MN, Lortal S.** 2006. Altering renneting pH changes microstructure, cell distribution and lysis of *Lactococcus lactis* AM2 in cheese made from ultrafiltered milk. J Dairy Sci **89:**812–823. http://dx.doi.org/10.3168/jds.S0022-0302(06)72144-0.
11. **Lopez C, Briard-Bion V, Camier B, Gassi JY.** 2006. Milk fat thermal properties and solid fat content in Emmental cheese: a differential scanning calorimetry study. J Dairy Sci **89:**2894–2910. http://dx.doi.org/10.3168/jds.S0022-0302(06)72562-0.
12. **Ercolini D, Hill PJ, Dodd CER.** 2003. Bacterial community structure and location in Stilton cheese. Appl Environ Microbiol **69:**3540–3548. http://dx.doi.org/10.1128/AEM.69.6.3540-3548.2003.
13. **Favrot C, Maubois JL.** 1996. Growth of *Lactococcus lactis* in milk and rennet curd: influence of the level of inoculation. Lait **76:**193–208. http://dx.doi.org/10.1051/lait:1996317.
14. **Jeanson S, Chadoeuf J, Madec MN, Aly S, Floury J, Brocklehurst TF, Lortal S.** 2011. Spatial distribution of bacterial colonies in a model cheese. Appl Environ Microbiol **77:**1493–1500. http://dx.doi.org/10.1128/AEM.02233-10.
15. **Le Boucher C, Courant F, Royer AL, Jeanson S, Lortal S, Dervilly-Pinel G, Thierry A, Le Bizec B.** 2015. LC-HRMS fingerprinting as an efficient approach to highlight fine differences in cheese metabolome during ripening. Metabolomics **11:**1117–1130. http://dx.doi.org/10.1007/s11306-014-0769-0.
16. **Bunthof CJ, Van Schalkwijk S, Meijer W, Abee T, Hugenholtz J.** 2001. Fluorescent method for monitoring cheese starter permeabilization and lysis. Appl Environ Microbiol **67:**4264–4271. http://dx.doi.org/10.1128/AEM.67.9.4264-4271.2001.
17. **Cretenet M, Laroute V, Ulve V, Jeanson S, Nouaille S, Even S, Piot M, Girbal L, Le Loir Y, Loubière P, Lortal S, Cocaign-Bousquet M.** 2011. Dynamic analysis of the *Lactococcus lactis* transcriptome in cheeses made from milk concentrated by ultrafiltration reveals multiple strategies of adaptation to stresses. Appl Environ Microbiol **77:**247–257. http://dx.doi.org/10.1128/AEM.01174-10.
18. **Le Boucher C, Courant F, Jeanson S, Chereau S, Maillard MB, Royer AL, Thierry A, Dervilly-Pinel G, Le Bizec B, Lortal S.** 2013. First mass spectrometry metabolic fingerprinting of bacterial metabolism in a model cheese. Food Chem **141:**1032–1040. http://dx.doi.org/10.1016/j.foodchem.2013.03.094.
19. **Lecomte X, Gagnaire V, Briard-Bion V, Jardin J, Lortal S, Dary A, Genay M.** 2014. The naturally competent strain *Streptococcus thermophilus* LMD-9 as a new tool to anchor heterologous proteins on the cell surface. Microb Cell Fact **13:**82. http://dx.doi.org/10.1186/1475-2859-13-82.
20. **Juillard V, Laan H, Kunji ERS, Jeronimus-Stratingh CM, Bruins AP, Konings VN.** 1995. The extracellular PI-type proteinase of *Lactococcus lactis* hydrolyses beta-casein into more than one hundred different oligopeptides. J Bacteriol **177:**3472–3478.
21. **Dalgleish DG.** 2011. On the structural models of bovine casein micelles—review and possible improvements. Soft Matter **7:**2265–2272. http://dx.doi.org/10.1039/C0SM00806K.
22. **Floury J, Jeanson S, Madec MN, Lortal S.** 2013. Porosity of *Lactococcus lactis* subsp. *lactis* LD61 colonies immobilised in model cheese. Int J Food Microbiol **163:**64–70. http://dx.doi.org/10.1016/j.ijfoodmicro.2013.02.014.
23. **Floury J, El Mourdi I, Silva JVC, Lortal S, Thierry A, Jeanson S.** 2015. Diffusion of solutes inside bacterial colonies immobilized in model cheese depends on their physicochemical properties: a time-lapse microscopy study. Front Microbiol **6:**366. http://dx.doi.org/10.3389/fmicb.2015.00366.
24. **Jeanson S, Floury J, Gagnaire V, Lortal S, Thierry A.** 2015. Bacterial colonies in solid media and foods: a review on their growth and interactions with the micro-environment. Front Microbiol **6:**1284.